# Comparative Study of the Tuning Performances of the Nominal and Long $L^*$ CLIC Final Focus System at $\sqrt{s}$ = 380 GeV

*F. Plassard*[*1,2], *A. Latina*[1], *E. Marin*[1] *and R. Tomás*[1]
[1] CERN, Geneva, Switzerland
[2] University Paris Sud, Orsay, France

**Abstract**
Mitigation of static imperfections for emittance preservation is one of the most important and challenging tasks faced by the Compact Linear Collider (CLIC) beam delivery system. A simulation campaign has been performed to recover the nominal luminosity by means of different alignment procedures. The state of the art of the tuning studies is drawn up. Comparative studies of the tuning performances and a tuning-based final focus system design optimization for two $L^*$ options are presented. The effectiveness of the tuning techniques applied to these different lattices will be decisive for the final layout of the CLIC final focus system at $\sqrt{s} = 380$ GeV.

**Keywords**
Linear collider; CLIC; final focus system; alignment; tuning; long $L^*$.

## 1 Introduction

The Compact Linear Collider (CLIC) rebaselining foresees a staged machine with an initial centre-of-mass energy of 380 GeV [1], for which the design optimization and tuning of the final focus system (FFS) is presented in this paper. The FFS aims to demagnify the beams down to the nanometre level. The small values of the $\beta$-functions at the collision point (Table 1) are provided by two strong quadrupoles (QF1 and QD0), with QD0 located at a distance $L^*$ from the interaction point (IP). Beam size growth, arising from chromatic and higher-order aberrations, is controlled by optics arranged according to the local chromaticity correction scheme [2]. The distance $L^*$ is planned to be 4.3 m [3] for the nominal lattice, forcing QD0 to be integrated inside the experiment and protected by an anti-solenoid, to avoid interplay between the quadrupole and the solenoid fields. Machine detector interface issues are removed with an alternative longer $L^*$ of 6 m [4] but one has to expect a reduction in the maximum luminosity achievable, owing to the increase in chromaticity propagated to the IP (Table 1).

*Corresponding author.

**Table 1:** CLIC 380 GeV design parameters for both $L^*$ options

| $L^*$ [m] | 4.3 | 6 |
|---|---|---|
| Final focus system length [m] | 553 | 770 |
| $\gamma\epsilon_x/\gamma\epsilon_y$ [nm] | 950/20 | 950/20 |
| $\beta^*_x/\beta^*_y$ [mm] | 8.2/0.1 | 8.2/0.1 |
| $\sigma^*_{x,\text{design}}$ [nm] | 145 | 145 |
| $\sigma^*_{y,\text{design}}$ [nm] | 2.3 | 2.3 |
| $L_{\text{tot, design}}$ [$10^{34}\,\text{cm}^{-2}\text{s}^{-1}$] | 1.5 | 1.5 |
| $L_{1\%\text{, design}}$ [$10^{34}\,\text{cm}^{-2}\text{s}^{-1}$] | 0.9 | 0.9 |
| Chromaticity $\xi_y$ ($\approx L^*/\beta^*_y$) | 43000 | 60000 |



https://doi.org/10.23727/CERN-Proceedings-2017-001.29

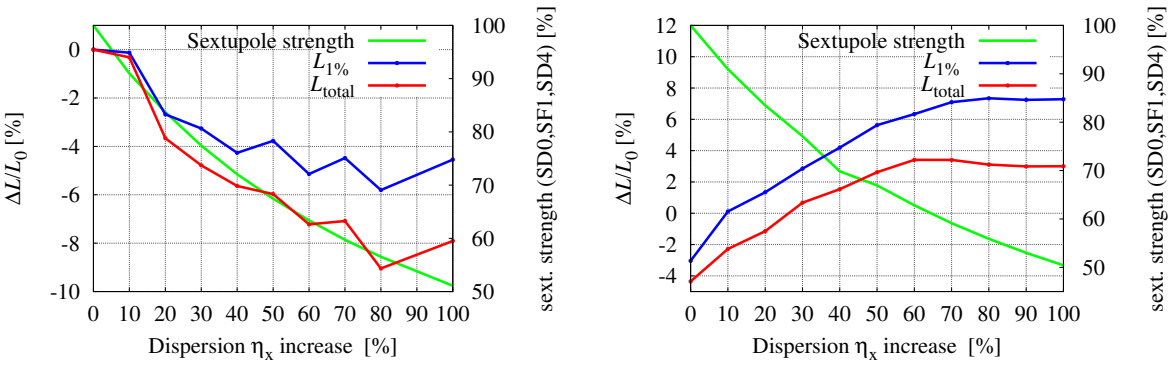


**Fig. 1:** Relative luminosity and average strength of the last three sextupoles versus dispersion increase through the final focus system. Left: $L^* = 4.3$ m; right: $L^* = 6$ m.

The small tolerances of the FFS on magnet position stability renders the luminosity tuning strategy very challenging. In the presence of realistic transverse magnet misalignments of a few micrometres, the luminosity can decrease by several orders of magnitude. It is thus necessary to prove that the proposed FFS lattice design fulfils the tuning requirements. The FFS designs have been optimized by targeting the optimal luminosity and momentum bandwidth of a perfectly aligned system. A first tuning simulation campaign, comparing both $L^*$ options, has demonstrated the need for changes in the FFS layout to increase the effectiveness of the luminosity tuning. In this paper, it is proposed to promote the tuning efficiency as a figure of merit for the design of our system.

## 2 Final focus system design optimization with $L^* = 4.3$ m and $L^* = 6$ m

Two optimized lattices with nominal and long $L^*$ have been proposed in previous studies [5] for the first stage of CLIC at $\sqrt{s} = 380$ GeV. The nominal beam delivery system layout was based on the $\sqrt{s} = 500$ GeV beam delivery system design planned in the old staging strategy [6]. A scan of the bending magnet angles of the FFS has been performed in both cases in order to find the optimal dispersion level by considering the total and peak luminosities of an error-free system. Sextupoles need to be coupled with dispersion to correct chromatic aberrations; their strengths can then be reduced by increasing the dispersion level in the FFS, as shown in Fig. 1. According to the scan results in Fig. 1, the optimum performances are found with no changes in the bending magnet angles for the $L^* = 4.3$ m option and with 70% of dispersion increase for $L^* = 6$ m. Details of the performances and the optimization process of the beam size at the IP including the effect of high order aberrations [7, 8] can be found in Ref. [5]. The resulting Twiss functions along the FFS are shown in Fig. 2.

## 3 Tuning algorithm applied

The tuning procedure aims to mitigate the effect of static displacements in the horizontal and vertical planes [9] of the quadrupoles, sextupoles, and beam position monitors of the FFS. This procedure utilizes beam-based alignment techniques [10, 11], to correct the beam orbit throughout the system, and sextupole tuning knobs, to combat the linear aberrations at the IP. In the tuning simulation discussed here, these optics are randomly misaligned with $\sigma_{\text{RMS}} = 10$ µm, according to the pre-alignment specification for the CLIC beam delivery system [12]. Magnet strength, tilt, and roll errors have not yet been implemented. Random misalignments are applied to 100 machines. The beam-based alignment begins with a one-to-one correction technique [13] that aims to steer the beam through the centre of each beam position monitor using transverse kickers. The effectiveness of the orbit correction is compromised by the misaligned beam position monitors, leading to a dispersive orbit. To remove the remaining dispersion deviations from the nominal dispersion profile along the FFS, the so-called dispersion-free steering

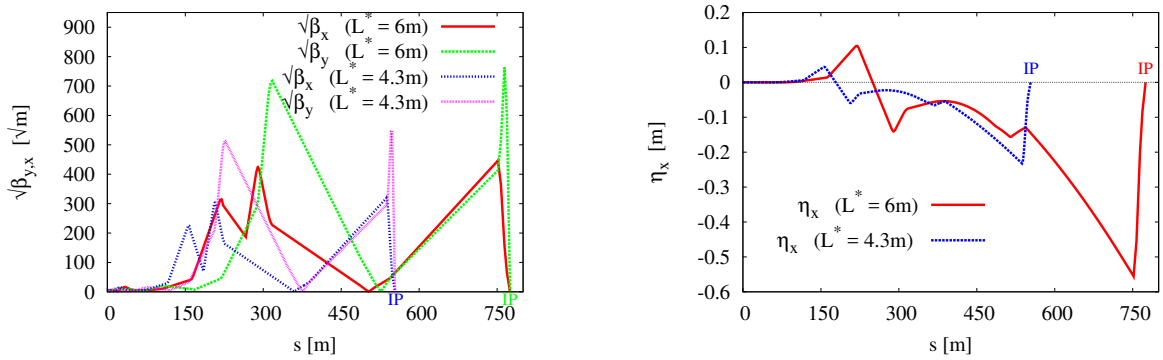


**Fig. 2:** Comparison of $L^* = 4.3$ m and $L^* = 6$ m after optimization. Left: Twiss functions $\beta_{x,y}$; right: dispersion $\eta_x$. IP, interaction point.

technique [14] is applied. The dispersion is evaluated by collecting two orbit readings, $x_{\Delta\vec{E}_+}$ and $x_{\Delta\vec{E}_-}$, of two beams, with energy deviations of $\pm\Delta E$. The dispersion is obtained as:

$$\vec{\eta} = \frac{x_{\Delta\vec{E}_+} - x_{\Delta\vec{E}_-}}{2\Delta E} \,. \tag{1}$$

The value of the corrector kicks $k_m$ for the correction of the orbit and dispersion is obtained by minimizing:

$$\chi^2 = \sum_{\text{BPMs}} x_i^2 + \omega^2 \sum_{\text{BPMs}} (x_{\Delta E,i} - x_i)^2 + \beta^2 \sum_{\text{Correctors}} k_m^2 \,, \tag{2}$$

where $i$ and $m$ are the indices of the beam position monitors and kickers, respectively. The weighting factors $\omega$ and $\beta$ are used to limit the value of the applied corrector kicks.

Linear aberrations at the IP created by the misaligned optics are corrected using pre-computed combinations of sextupole displacements in the transverse plane. Each set of sextupole knobs is constructed to be orthogonal, so that the chosen aberrations are corrected independently. Horizontal and vertical sextupole offsets $\Delta x$ and $\Delta y$ introduce feed-down normal and skew quadrupole fields (Eqs. (3) and (4)), which create distortions in the $\beta_{x,y}$ and $\eta_{x,y}$ functions and introduce betatron coupling at the IP:

$$\Delta B_x = B\rho\big[(k_2\Delta x)y + (k_2\Delta y)x + k_2\Delta x\Delta y\big] \,, \tag{3}$$

$$\Delta B_y = B\rho\left[(k_2\Delta x)x - (k_2\Delta y)y + \frac{1}{2}k_2\left(\Delta x^2 - \Delta y^2\right)\right] \,, \tag{4}$$

with

$$\Delta k_{1\mathrm{n}} = k_2\Delta x, \qquad \Delta k_{1\mathrm{s}} = k_2\Delta y \,, \tag{5}$$

where $B\rho$ is the magnetic rigidity, $k_2$ is the normalized sextupole strength, $k_{1\mathrm{n}}$ and $k_{1\mathrm{s}}$ are the normalized normal and skew quadrupole strengths, respectively. Knobs for shifting the waist position $\Delta\omega_{x,y}$ and horizontal dispersion $\Delta\eta_x^*$ aberrations are constructed by moving the sextupoles in the horizontal plane. Vertical dispersion $\Delta\eta_y^*$ and coupling aberrations are corrected using the vertical displacement of the sextupoles [15,16] . As the knobs are not fully orthogonal, one must scan the knobs iteratively to increase the luminosity further. In the tuning procedure applied here, the set of knobs is scanned twice with a large knob amplitude and twice with a smaller amplitude for better determination of the optimal luminosity. Finally, we define the four tuning steps as the first iteration of the linear knobs:

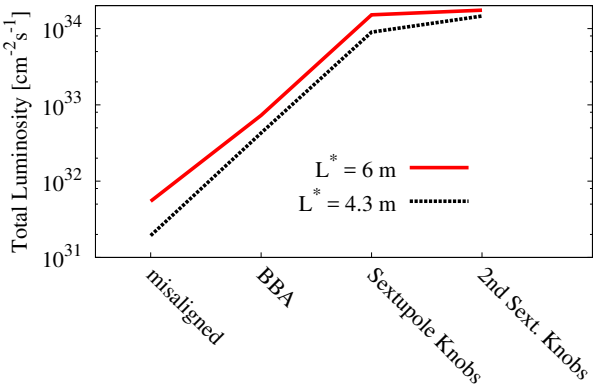


**Fig. 3:** Average luminosity over 100 machines after each tuning step for the two $L^*$ options of the final focus system optimized in Ref. [5]. BBA, beam-based alignment.

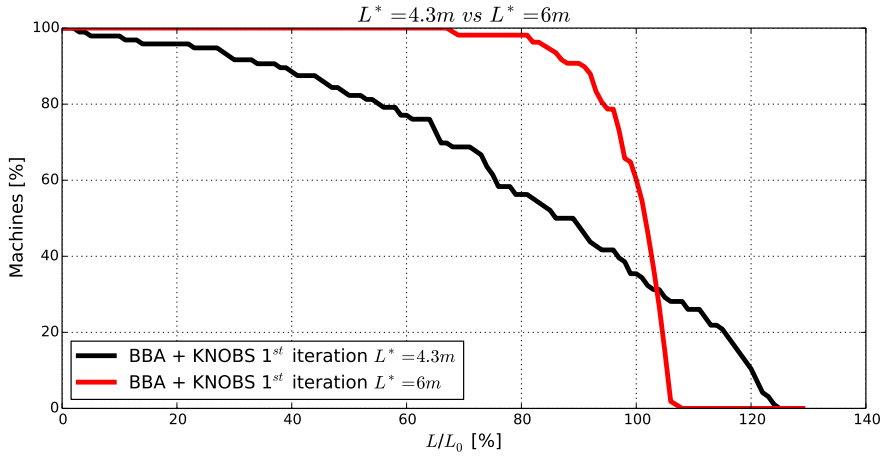


**Fig. 4:** Tuning simulation results of 100 machines achieving $L/L_0$ for the two $L^*$ options of the final focus system optimized in Ref. [5]. BBA, beam-based alignment.

1. one-to-one correction;
2. dispersion-free steering;
3. sextupole knob tuning;
4. second iteration of linear knob tuning.

## 4 Tuning simulation results

### 4.1 Final focus system tuning comparison: nominal versus long $L^*$

The following tuning simulations were applied on the optimized designs of the nominal and long $L^*$ options presented in Section 2. The average results at each tuning iteration, for the four tuning steps described in Section 3, are compared for both lattices in Figs. 3 and 4. One can see that the luminosity, after beam-based alignment and linear knob tuning, is better recovered for the $L^*$ = 6 m case, thanks to higher luminosity after transverse optics misalignments, as shown in Fig. 3.

To quantify the tuning effectiveness, one must consider the number of machines that recover the design luminosity ($L_0$ = 1.5 $\times 10^{34}\,\mathrm{cm}^{-2}\mathrm{s}^{-1}$). As shown in Fig. 4, for $L^* = 4.3$ m, only 35% of the

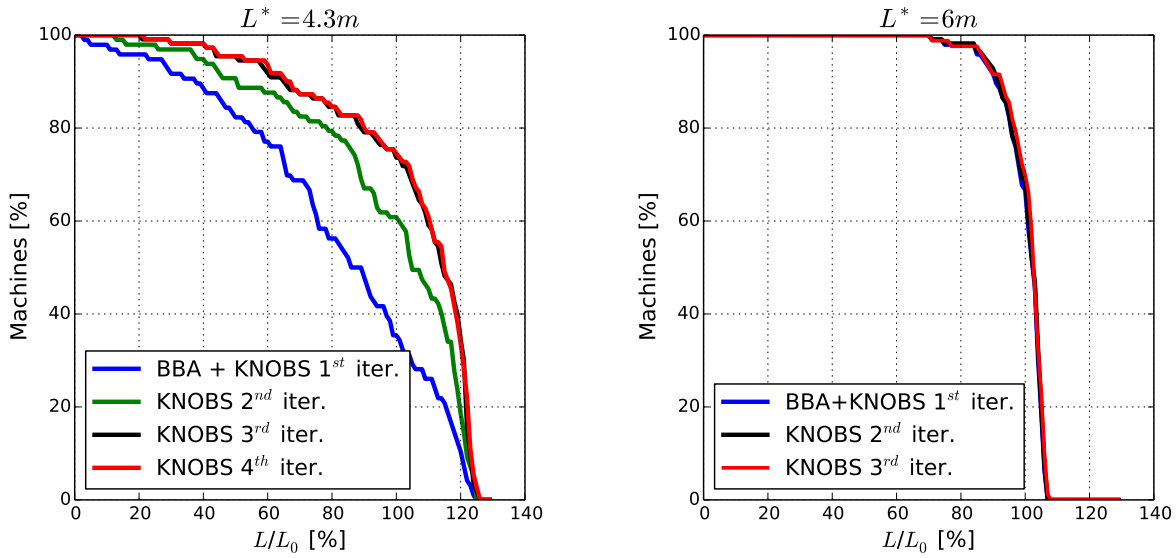


**Fig. 5:** Tuning simulation results of 100 machines achieving $L/L_0$ for the final focus system optimized in Ref. [5] after several iterations of the linear knobs. Left: $L^* = 4.3$ m; right: $L^* = 6$ m.

machines achieve $L_0$, compared with 60% for $L^* = 6$ m after the first iteration of the knobs. Despite a smaller achievable maximum luminosity, the long $L^*$ option shows better tuning efficiency than the nominal one. This can be improved by applying iterations of linear knobs until no further increase of the luminosity is observed. However, the tuning time is also a concern, owing to the impact of ground motion. Here, one iteration of linear knobs corresponds to ≈720 luminosity measurements. Figure 5 compares the luminosity increase after several knob iterations applied to both designs. The impact of the linear knobs reaches its limit after the third iteration for $L^* = 4.3$ m, with 75% of the machines achieving $L_0$. For $L^* = 6$ m, the limit is reached at the second iteration, with 70% of the machines recovering the design luminosity.

### 4.2 Tuning-based design optimization

From the comparative study described in Section 4.1, one may suspect that the tuning efficiency could be improved by optimizing the dispersion level in the FFS. The design optimization strategy applied in this study involves tuning a set of FFS lattices with different bending magnet angles. The tuning results of the dispersion scan will help to decide the optimal layout that maximizes the luminosity and tuning effectiveness.

All lattices have been randomly misaligned by $\sigma_{\text{RMS}} = 10$ μm in the transverse plane. When the sextupoles are displaced horizontally, feed-down normal quadrupole kicks are generated and the corresponding changes in the IP spot size are evaluated by:

$$\Delta\sigma_x^* = k_s \Delta_x \beta_{x,s} \sigma_{x0}^* \,, \tag{6}$$

$$\Delta\sigma_y^* = k_s \Delta_x \beta_{y,s} \sigma_{y0}^* \,, \tag{7}$$

where $\beta_{x,s}$ and $\beta_{y,s}$ are the $\beta$-functions at the sextupole location. Vertical sextupole displacements generate skew quadrupole kicks that increase the spot size by

$$\Delta\sigma_y^* = k_s \Delta_y \sigma_{x,s} \left| R_{34}^{s\to *} \right| \,, \tag{8}$$

where $\sigma_{x,s}$ is the horizontal beam size at the sextupole location and $R_{34}^{s\to *}$ is the matrix element from the sextupole to the IP. As a consequence of the chromatic correction, the strength of sextupoles $k_2$

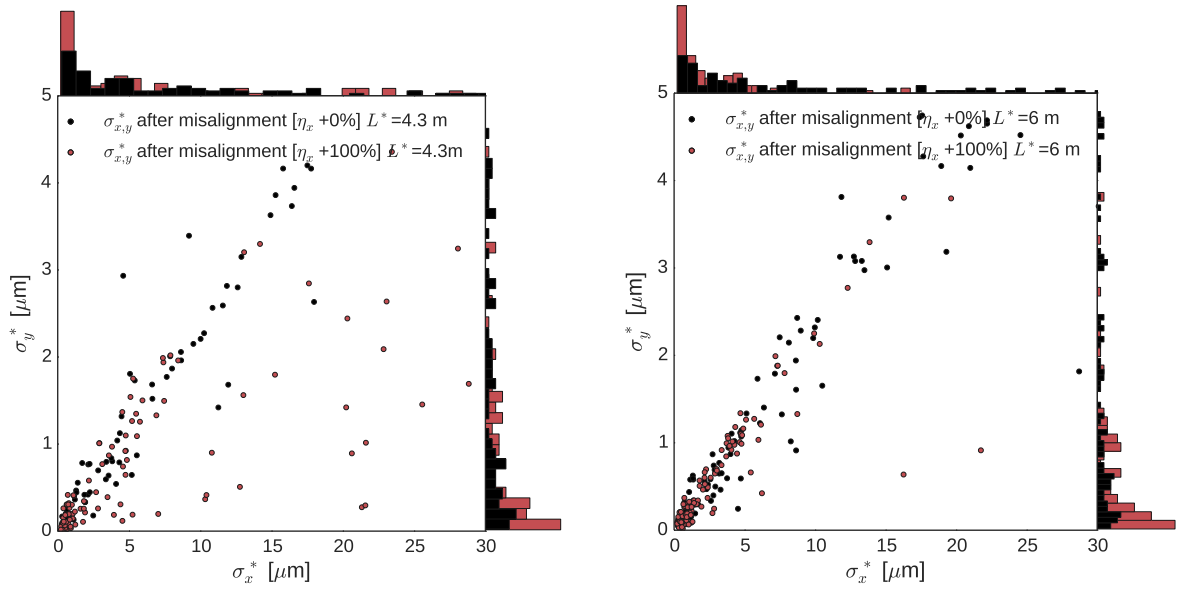


**Fig. 6:** Comparison of beam size distribution at the interaction point after misalignment of the magnets for two scenarios, 0% and 100% dispersion increase. Left: $L^* = 4.3$ m; right: $L^* = 6$ m. Histograms of $\sigma^*_{x,y}$ are plotted on mirror axes.

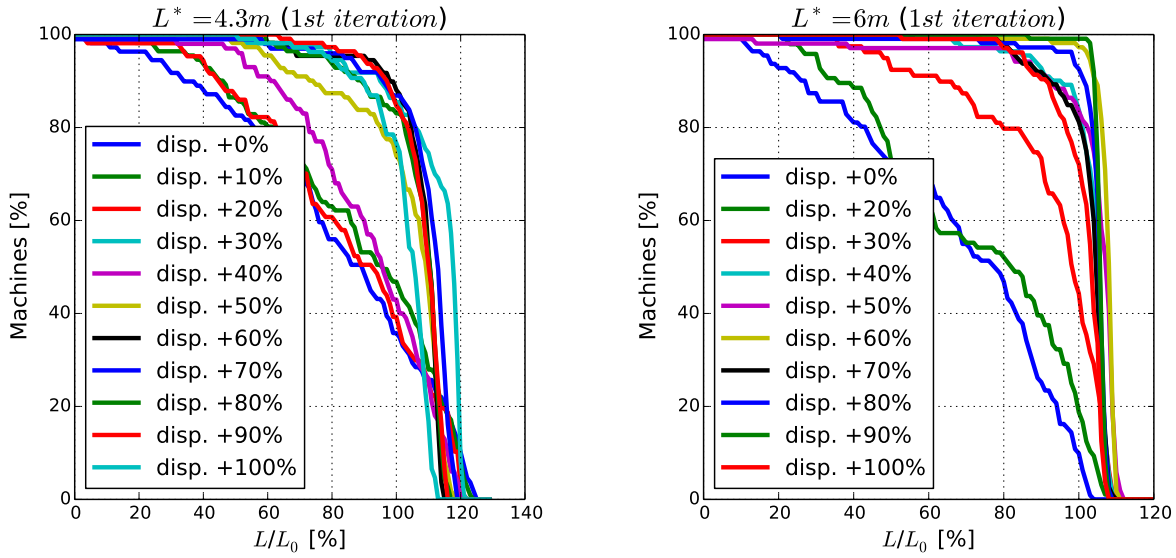


**Fig. 7:** Tuning effectiveness comparison between different dispersion levels from 0% to 100% increase. Left: $L^* = 4.3$ m; right: $L^* = 6$ m.

decreases when dispersion is increased, as shown in Fig. 1. From Eqs. (6)–(8), one can see that the impact of the sextupole misalignments on the beam size at the IP is reduced when $k_2$ decreases. In Fig. 6, the comparison of the beam sizes of the 100 machines after misalignment shows how the lattice becomes more tolerant to misalignment with an increase of dispersion in the FFS by a factor of two. A tuning simulation campaign has been performed on lattices with dispersion level intervals of 10% for the nominal and long $L^*$ options; the results are presented in Fig. 7.

Increasing the dispersion level by 60% results in an increase in the number of machines that achieve $L_0$, from 35% to 88% with only a 7% loss of maximum luminosity achievable for $L^* = 4.3$ m.

Increasing the dispersion by 20% (from +70% to +90%) results in 99% of the machines recovering $L_0$ with almost no loss in luminosity, considering an error-free lattice.

## 5 Conclusions

Optimizing the FFS by targeting the luminosity of an error-free lattice is not sufficient to prove its feasibility. Introducing tuning effectiveness as a new figure of merit for the design optimization is a more realistic approach in evaluating the performances of FFSs. It has been shown that reduction of the sextupole strengths is very helpful for tuning the machine, especially in the nominal $L^*$ case, where the tuning performance has been significantly improved. More tuning iterations of the new optimized lattices are needed in order to determine the final layout of the FFS for both $L^*$ options. One must balance between maximum luminosity achievable and tuning time, according to the need of the machine during operation.

## References


[1] P. Burrows (CLIC Accelerator Collaboration), CLIC accelerator: status, plans and outlook, CLIC Workshop, CERN, Geneva, 2016.

[2] P. Raimondi and A. Seryi, *Phys. Rev. Lett.* **86** (2001) 3779. http://dx.doi.org/10.1103/PhysRevLett.86.3779

[3] A Multi-TeV Linear Collider Based on CLIC Technology: CLIC Conceptual Design Report, CERN-2012-007 (CERN, Geneva, 2012). https://doi.org/CERN-2012-007

[4] A. Seryi, Near IR FF design including FD and longer $L^*$ issues, CLIC08 (2008).

[5] F. Plassard *et al.*, CLIC beam delivery system rebaselining and long $L^*$ lattice optimization, TH-PMR045 Proc. IPAC2016, Busan, Korea, 2016.

[6] R. Tomas *et al.*, The CLIC BDS towards the conceptual design report, SLAC-PUB-15156 (2010).

[7] R. Tomas. *Phys. Rev. ST Accel. Beams* **9** (2006) 081001. http://dx.doi.org/10.1103/PhysRevSTAB.9.081001

[8] R. Tomas *et al.*, CLIC final focus studies, Proc. EPAC 2006, Edinburgh, Scotland, 2006.

[9] B. Dalena *et al.*, *Phys. Rev. ST Accel. Beams* **15** (2012) 051006. http://dx.doi.org/10.1103/PhysRevSTAB.15.051006

[10] P. Tenenbaum and T. O. Raubenheimer, *Nucl. Instrum. Methods Phys. Res. A* **302** (1991) 191. http://dx.doi.org/10.1016/0168-9002(91)90403-D

[11] A. Latina *et al.*, Alignment of the CLIC BDS, CERN-AB-2008-011; CLIC-Note 753, (CERN, Geneva, 2008).

[12] H. Mainaud Durand *et al.*, Alignment challenges for a future linear collider, IPAC13, Shanghai, 2013, WEPME046.

[13] Y. Chung *et al.*, Closed orbit correction using singular value decomposition of the response matrix, Particle Accelerator Conf., Dallas, Texas, 1993.

[14] C. Fischer and G. Parisi, Trajectory correction algorithms on the latest model of the CLIC main LINAC, CERN-SL-96-065-BI, CLIC Note 315, (CERN, Geneva, 1996).

[15] Y. Nosochkov *et al.*, Tuning knobs for the NLC Final Focus, Proc. EPAC 2002, Paris, 2002.

[16] T. Okugi *et al.*, *Phys. Rev. ST Accel. Beams* **17** (2014) 023501. http://dx.doi.org/10.1103/PhysRevSTAB.17.023501